

Classification and Segmentation of COVID-19 from chest CT image using Deep Learning

¹Prabhakar Singh, ²Shashidhar R. Joshi

*Department of Electronics and Computer Engineering
Pulchowk Campus, Tribhuvan University, Lalitpur, Nepal
1Rajput.prabhakaran@gmail.com, 2 srjoshi@ioe.edu.np*

Abstract

Deep Learning based classification and segmentation of medical imaging data, with special attention to the COVID-19 virus, is a desperately required application. The lives of millions of individuals are being impacted by this pandemic issue.

The most frequent result that involves expert evaluation in COVID-19 computed tomography (CT) images of the lungs is ground glass turbidity. In light of this circumstance, some researchers suggest the appropriate deep learning models that, in the absence of trained diagnostic professionals in health centers, can serve as an alternative. Thus, the patient's CT images are categorized into three groups using the algorithm: COVID-19, CAP (Community Acquired Pneumonia), Normal, all with an assured high level of accuracy. The next step involves the use of two datasets for segmentation and classification. Using an image enhancement technique known as CLAHE (Contrast Limited Adaptive Histogram Equalization), noise and intensity uniformity were removed in this project. Normalization of the data and annotation reduce the constraint of a small dataset and expand the dataset size. ResNet50, VGG16 and Densenet169 architectures are used for transfer learning and yield the accuracy during classification are 95.94 %, 94.79 % and 97.00% respectively. Semantic segmentation and Instance Segmentation of medical images has been done where we got Dice value of 0.7348.

Keywords: Classification, Segmentation, VGG-16, Resnet50, Dense net 169, Accuracy, ROC, Dice Score

1. INTRODUCTION

A major global health emergency has been created by the coronavirus disease 2019 (COVID-19), which spread over the globe toward the end of 2019. Our lives and health are in grave danger due to its fast spread. On December 1, 2022, the total number of confirmed COVID-19 cases worldwide hit 648.50 million, according to World meters' global real-time

Statistics. A total of 6.642 million people died, reaching 6,642,534. Analyzing samples that show the presence or absence of the severe acute respiratory syndrome-associated coronavirus 2 (SARS-CoV-2) during COVID-19 testing. The test is performed to find out whether the virus is present or whether antibodies created in response to infection are present. The COVID-19 diagnostic technique can be broadly divided into two groups: a laboratory-based approach, which includes point-of-care testing, nucleic acid testing, antigens tests, and serology (antibody) tests. The alternative strategy involves using medical imaging diagnostic techniques including computed tomography (CT) and X-rays. [1]. RT-PCR is laboratory-based tests are performed on samples obtained via nasopharyngeal swab, throat swabs, sputum, and deep airway material [2]. The most common diagnostic approach is the nasopharyngeal swab, which involves exposing a swab to paper strips containing artificial antibodies designed to bind to coronavirus antigens. Antigens bind to the strips and give a visual readout [1]. The process is pretty fast and is employed at the point of care. The nucleic acid test has low sensitivity between 60-71 % [2].

Environmental elements like specimen sampling, the detection process, and the detection reagent have an impact on nucleic acid detection methods. This procedure typically produces some false positives and requires an excessively long wait for results. The case summaries reveal that imaging characteristics of patients with COVID-19 can also be used as a diagnostic criterion. The use of CT, a

practical and sophisticated medical imaging tool, is crucial in the diagnosis of COVID-19. While CT imaging is useful for the diagnosis of COVID-19, reading the scans manually is time-consuming and subject to human errors [3]. Therefore, advanced artificial intelligence (AI)-based automated image analysis is demanded to analyze CT scans in the assessment of COVID-19. AI-based image analysis methods can provide accurate and rapid diagnosis of the disease to cope with the demand for a large number of patients. For example, a manual assessment of a CT scan can take up to 15 min, while AI-based image analysis requires only a few seconds. Further, to alleviate the burden of medical professionals in reading CT scans, several works have developed deep learning methods that can automatically interpret CT images and predict whether the CT scans show positive or not for COVID-19 [3].

2. LITERATURE REVIEW

High-resolution medical images are created during a CT scan by passing X-rays into the patient's chest, and these images are then detected by radiation detectors [2]. Medical imaging, such as computed tomography (CT), has become crucial in the global fight against COVID-19, and recently emerging artificial intelligence (AI) technologies are boosting the power of imaging tools and supporting medical professionals [1]. CT imaging appears to be used for respiratory issue diagnosis. Lung diseases may be recognized and categorized by doctors using the data from the segmentation of organs and tumors in chest CT slices. The difficulty in obtaining testing kits and ventilators limits the ability to quickly and accurately screen for COVID 19. Additionally, false negative rates for RT-PCR testing have been recorded [4].

Imaging methods, such as computed tomography (CT) and X-rays, have been used for detection as a supplement to RT-PCR assays [2]. Due to its three-dimensional perspective of the lung, CT screening is favored over X-rays. In recent investigations [4], the usual indications of infection, such as ground-glass opacity (GGO) in the initial phase and lung consolidation in the late stage, may be seen from CT slices. To differentiate COVID-19 patients and normal, Wang et al. presented an inception neural network [5].

Song et al. [6] implemented Medical screening of CT images using deep learning to diagnose COVID-19, to predict disease and feature extraction using fuzzy model. Fuzzy models related work area is image classification, Fuzzy decision system, Feature extraction and selection. The accuracy obtained by this model is 94.2% and its F1 score is 93.8%. Ko et al. [7] suggested a framework, a fast-track COVID-19 classification network (FCONet), that employs VGG16, ResNet-50, InceptionV3, and Xception as a framework to classify images as COVID-19, other pneumonia, or non-pneumonia. They included 1194 COVID-19, 264 low-quality COVID-19 (only for testing), and 264 additional COVID-19 scans in their study together with 2239 CT scans for pneumonia, ordinary, and other diseases. Each image was converted to a 256 by 256 grayscale version. They applied data augmentation techniques including data rotation and data zoom to boost the number of training examples. FCONet based on ResNet50 surpassed other pre-trained models and achieved 96.97% accuracy in the independent test data set of COVID-19 pneumonia image. Positive and negative COVID-19 picture identification Salma et al. [3] established a paradigm for segmenting and classifying CT images.

To classify CT images, many models, including ResNet50 and VGG16, are employed. The most widely used deep l

earning architecture for image segmentation, U-Net, is combined with ResNet50 and VGG16 to improve system performance. To enhance photo preparation methods, employ the Wiener filter and image size dependent normalization technique (ISDNT). The dataset is derived from COVID-19 lung CT scans, and Kaggle is used to implement the suggested architectures, which include end-to-end VGG16, ResNet50, and U-Net with VGG16 or ResNet50. U-Net hybrid with ResNet50 yields the greatest results. The suggested classification model's accuracy (ACC) is 98.98%, and its area under ROC curve of 98.87 Using transfer learning that was based on DenseNet201, Jaiswal et al. [8] employed COVID-19 for the identification and diagnosis. The effectiveness of DenseNet201 was assessed using 2492 chest CT-scan images (1262 with COVID-19 and 1230 healthy), and metrics for precision, F1-measure, specificity, sensitivity, and accuracy. In comparison to VGG16, Resnet152V2, and InceptionResNet, quantitative results showed precision=96.29%, F1-measure=96.29%, specificity=96.29%, sensitivity=96.21%, and accuracy=96.25 %, numbers indicating the efficacy of the model. Ahuja et al. [9] used pre-trained networks and data augmentation to arrange COVID-19 pictures. Using stationary wavelets for data augmentation, the randomized rotation, translation, and shear operations had been applied to the CT scan images. ResNet18 outperformed other models, obtaining an AUC score of 0.9965 in Ahuja et al. classification's challenge, which used ResNet18, ResNet50, ResNet101, and Squeeze Net.

3 METHODOLOGY

Methodology divided into 2 parts, one is classification and other is segmentation. First part as classification contains different Phases: Dataset, Pre-processing, transfer learning, classification performance metrics [3]. The proposed work techniques are to classify CT images into Normal, CAP (Community-Acquired Pneumonia) and COVID-19 and then segmentation using U-Net Architecture.

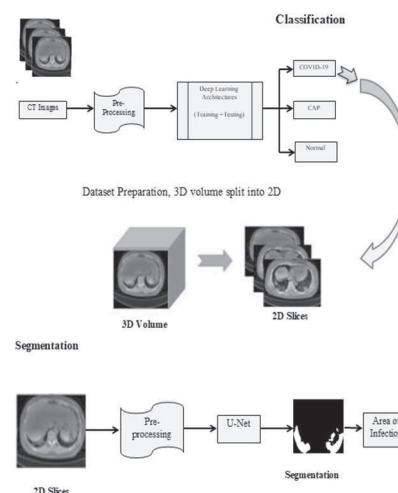


Fig 1: Block diagram Methodology

A. Dataset

The COVID-19 CT scan images dataset was collected from kaggle [10], [11]. For study on COVID-19, several datasets have been created and made accessible to researchers, physicians, and data scientists. Dataset with three different kinds of CT scans: Normal, COVID-19, and CAP. Data source is managed by Core COVID-Net Team, the team members are from different countries and organizations like DarwinAI Corp., Canada and Vision and Image Processing Research Group, University of Waterloo, Canada.

For segmentation of COVID-19 dataset, the dataset of chest CT images in .nii format, i.e. in 3D form of image, is labeled as original CT image, lungs mask, and infection mask. The original dataset of chest CT images for classification is in PNG format for COVID-19, CAP, and Normal with resolution 512*512 pixels. Total number of images contained in the dataset is 14868. The split ratio of the data set used for classification is 70:30 and segmentation is 0.8:0.2. CSV files are used to convey image tagged data for segmenting the whole dataset. Total number of image slice generated for segmentation is 2112 form from 3D CT scan.

Table 1: Split ratio of dataset used for classification is 70:30

Class	Training Dataset	Testing Dataset	Total
COVID-19	3577	1472	5049
CAP	3456	1563	5019
Normal	3374	1426	4800
Total	10407	4461	14868

B. Preprocessing

In the proposed algorithm, enhancing the image contrast and denoising are applied as the preprocessing step for the CT lungs images. This step is performed to improve the images quality and therefore increase the images identification [3]. Under preprocessing, image resizing, image enhancement is done. Here image preprocessing refers to scaling of image dataset to required pixels (224*224). Enhancement technique known as CLAHE.

C. Data augmentation and Transfer learning Phase

Data augmentation is the technique of increasing the quantity of data; in fact, we don't need to acquire new data instead, we just need to change the data that is already there. Since deep learning requires more data that is always practical to obtain, data augmentation becomes an option. The size of the data set can be expanded. Data augmentation is done by transformation method- Zooming, Rotation, Shearing, Flipping, Cropping.

In the data augmentation phase, all CT scan images are transformed to a single format (.PNG), resized in order to meet the requirements of the transfer learning-based model, and then normalized in [0,1] to ensure uniformity.

Transfer learning refers to the process of adopting previously acquired knowledge to new contexts. Rather using model from scratch, it's better to use pre-train model to achieve higher performance. A large number of datasets are needed while training from scratch. However, adopting pre-trained models

speeds up our proposed methods and saves time. Using previously trained models by altering their parameters.

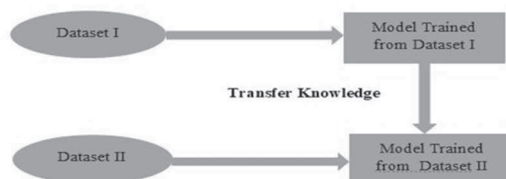


Fig 2: Transfer Learning Block Diagram

Here the knowledge gain after model train from dataset I that is apply on dataset II ,this is why it is known as pre-trained model .There are various types of Transfer Learning models as:

- ResNet50 based Architecture
- DenseNet169 based Architecture
- VGG-16 based Architecture

D. Architecture for Classification and Segmentation

ResNet50 based Architecture

To address the problem, ResNet Architecture introduces residual learning to overcome gradient and precision drop in training sets, ResNet. This allows the network to become deeper while ensuring accuracy and limiting speed. Convolutional layer and Polling layer stacking in this ResNet architecture degrades network performance because gradients become zero or unusually big. To address this issue, connection is utilized, which essentially allows for layer skipping or adding more layers. The purpose of employing skip connections is to lessen overfitting and training and testing mistake. ResNet50, ResNet101, and ResNet152 are other models in the ResNet series. [12].

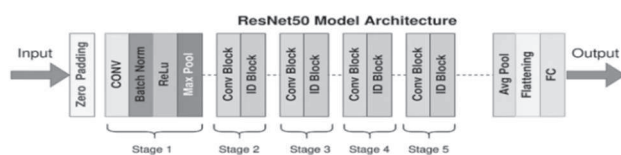


Fig 3: Resnet50 Architecture

DenseNet169 based Architecture

Huang et al. [13] uses DenseNet model, Dense Block (DB), the transition layer, and the growth rate represent the majority of the DenseNet model’s core. A series of devices under the DenseNet brand include the DenseNet121, DenseNet169, DenseNet201, and DenseNet264. DenseNet169 has the

advantage of requiring plentiful features, allowing for the training of deeper models during computation. Additionally, the fully connected layer of the model also has a regularization effect, which can help prevent overfitting on smaller datasets. The network architecture of DenseNet169, which has 338 depth and 12,487,810 parameters.

VGG-16 based Architecture

Simonyan and Zisserman were the ones who first proposed the VGG network architecture. The Visual Geometry Group (VGG) team submitted their ImageNet Challenge 2014 submission using the VGG models with 16 layers (VGG-16) and 19 layers (VGG19), which led to first and second place, finishes in the localization and classification categories, respectively. Convolution neural network that is frequently employed for image classification tasks is VGG-16. VGG-16 supports 224×224 pixel input images. It has a total of 21 layers, including three dense layers, five Max pooling layers, and 13 convolution layers. VGG-16 consists of 16 weighted layers. VGG-16 is made up of series of Convolutional layer, Max pooling layer, fully connected dense layers, and Softmax layer. Filter size for the convolution layer is 3×3 , and stride and padding are both set to 1. The maximum pooling layer features a filter with a 2×2 filter size, a stride of 2, and no padding.

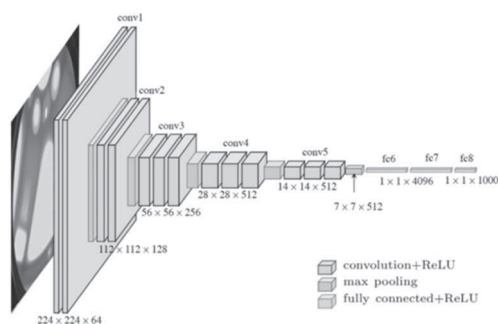


Fig 4: VGG-16 Architecture

E. Classification

The models utilized by Salama et al. [3] were ResNet50 and DenseNet, and they performed the classification procedure at its best. To be usable as the input for the suggested models, the greyscale CT lung pictures are scaled to the appropriate pixel sizes. Here main goal is to classify the CT scans images into Normal, COVID-19, and CAP using different transfer learning Resnet50, VGG-16 and Densenet169 with better accuracies.

F. Model Evaluation

The accuracy of any machine learning model's predictions seems to be determined how effective it is. The following performance evaluation measures are used to rate the effectiveness of the suggested model. Accuracy: This metric measures the percentage of correctly identified cases relative to the entire dataset. The ML algorithm performs better if the accuracy is higher. Accuracy is a significant measure for a test dataset that includes a balanced class. It is computed as follows:

$$Accuracy = \frac{(TP+TN)}{(TP+TN+FP+FN)} \quad (1)$$

Specificity: Specificity measure the model's capability to determine the true negatives of each available class.

$$Specificity = \frac{TN}{(TN+FP)} \quad (2)$$

Precision: This metric is a measure of exactness, which is calculated as the percentage of positive predictions of COVID-19 that were true positives divided by the number of predicted positives. It is computed as follows:

$$Precision = \frac{TP}{(TP+FP)} \quad (3)$$

Recall: This metric is a measure of completeness, which is calculated as the percentage of positives that were correctly identified as true positives divided by the number of actual positives. It is computed as follows:

$$Recall = \frac{TP}{(TP+FN)} \quad (4)$$

F-measure: This is a combination of precision and recall that provides a significant measure for a test dataset that includes an imbalanced class. It is computed as follows:

$$F \text{ -measure} = 2 * \frac{(Precision*Recall)}{(Precision+Recall)} \quad (5)$$

Where TP,TN, FN and FP represents as COVID-19 sample correctly classified ,NON-COVID-19 sample correctly classified ,NON-COVID sample classified as COVID-19 and COVID-19 sample classified as non-COVID-19 [14].

Space under the curve Area under the ROC curve, sometimes referred to as AUC, is a two-dimensional measurement of the ROC curve [15]. AUC for the optimum model is 1. The accuracy of the model's predictions will be higher the higher the AUC number. ROC curves are typically employed when a binary classification issue arises. Three classes on the ROC curve are involved in our issue. Three ROC curves were plotted separately and together as well.

Dice Coefficient, often referred to as Dice Score, is an estimate of how well a prediction matches the actual data, giving the intersection of the two additional significance. Its value spans from 0 to 1 , and the greater the value, the more accurate the segmentation. It is stated in Equation (6):

$$Dice = \frac{2TP}{(2TP+FP+FN)} \quad (6)$$

G. Segmentation

One of the most important steps in order to interpret CT scans, the region of interest (ROI) for early detection by using the segmentation Salama et al. [3] uses each pixel in the dataset is classified as either a ROI or a background during segmentation. For biomedical segmentation model the U-Net neural is very popular, for the analysis of biomedical images. In binary image segmentation contests, such as medical image analysis, satellite image analysis and others, this architecture has thus far demonstrated its effectiveness.

The encoder and decoder are the two main components of a U-Net model's overall architecture. Data is captured via the encoder component, which uses a CNN's standard design of alternating convolution and pooling processes. The decoder component responsible for the segmentation mask of the images by employing transposed convolution (deconvolution) processes to decode the information, enabling exact localization.

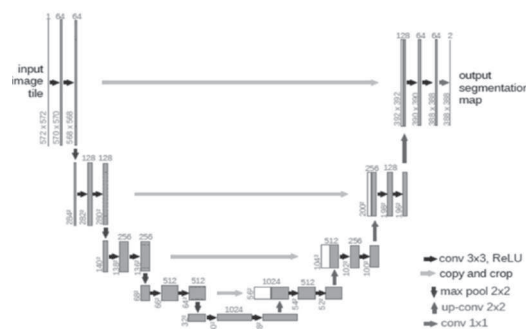


Fig 5: U-Net Architecture

Interest including the lungs. The contour (largest Closed Boundary) with the largest area would be the contour containing the lungs. For this reason, we decided to crop just the ROI that encompasses the lungs.

4. RESULT AND ANALYSIS

In this work, the models are able to classify into 3 different classes from Chest CT images. Total data is split into ratio 70:30 ,for training 10,407 images were trained and 4461 were validated .For segmentation 20 CT scan images are taken from those CT scan 2112 image slices are used by converting 3D images to 2D images. In the images it consists of different labels like original CT images ,infection mask ,lung mask .U-Net is utilize for segmentation and the original CT images are compared with lungs and infection mask present in dataset. The data were split into 80:20 for Training and Validation. The result is provided in from of dice. After getting the result of prediction we can calculate the area of ROI (Region of Interest) or area of infection.

4.1 Classification

4.1.1 Comparison of Accuracy and Loss curve obtains from Training vs Validation of different architectures.

Training and validation dataset is same for four Models where the images belonging to 3 classes. Batch Size 32 is considered for four deep learning models are same but the dropout are different for different models. All model got accuracy with different epoch numbers.

Table 2: Different Model with their Accuracy

Model Architecture	Input Size	Epochs	Accuracy
ResNet50	224*224	25	95.94 %
VGG16	224*224	25	94.79 %
DenseNet169	224*224	30	97.00 %

Figure 6 Training Vs Validation run for 25 epochs with Resnet50 Architecture and the graph validate the accuracy of 95.94% and loss of 4.06%.,

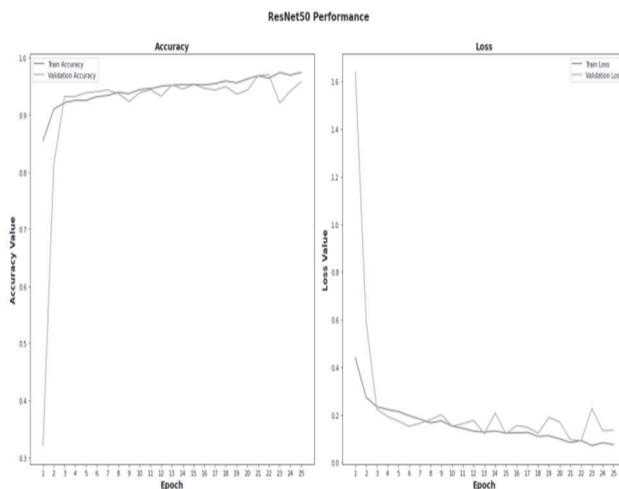


Fig 6: Training Vs Validation Accuracy and Loss based on ResNet50 model.

Figure 7 Training Vs Validation run for 25 epochs with VGG-16 Architecture and the graph validate the accuracy of 94.79%.and loss of 5.21%.,

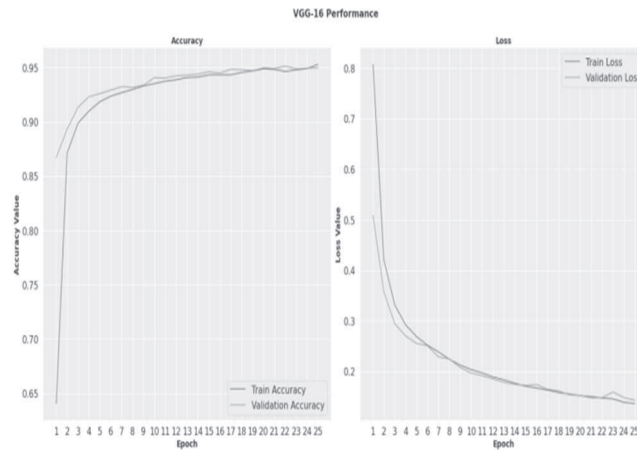


Fig 7: Training Vs Validation Accuracy and Loss based on VGG-16 model

Figure 8 Training Vs Validation run for 30 epochs with DenseNet169 Architecture and the graph validate the accuracy of 97.00% and loss of 3.0%.

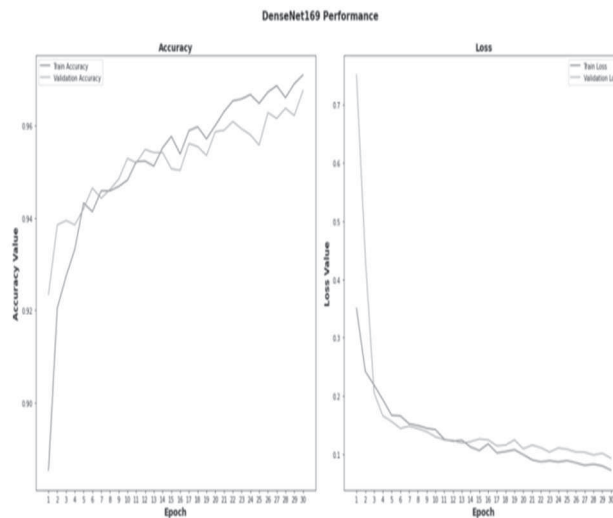


Fig 8: Training Vs Validation Accuracy and Loss based on DenseNet169

4.1.2 Comparison of ROC curve of different architectures.

Figure 9 shows ROC curve run for 25 epochs with Resnet50 Architecture where class 0 represented as Normal, class 1 represented as CAP and class 2 represented as Covid-19 and AUC scored from multiple classes, class 0=0.97, class 1=1.0 and class 2=0.94,

Figure 10 shows ROC curve run for 25 epochs with VGG-16 Architecture where class 0 represented as Normal, class 1 represented as CAP and class 2 represented as Covid-19 and AUC scored from multiple classes, class 0=0.96, class 1=1.0 and class 2=0.93.,

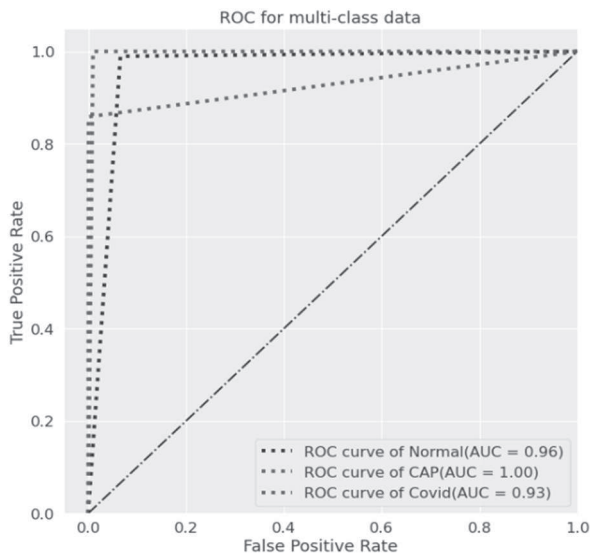


Fig 9: ROC curve based on Resnet50 model

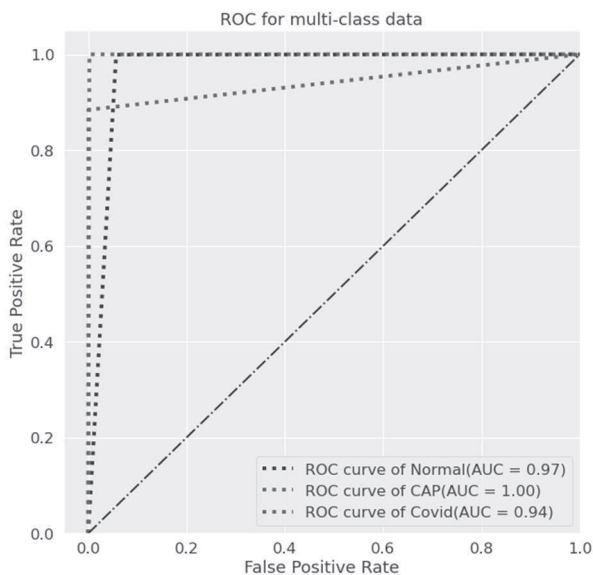


Fig 10: ROC curve based on VGG-16 model

Figure 11 shows ROC curve run for 30 epochs with Densenet169 Architecture where class 0 represented as Normal, class 1 represented as CAP and class 2 represented as Covid-19 and AUC scored from multiple classes, class 0=0.97, class 1=1.0 and class 2=0.96.

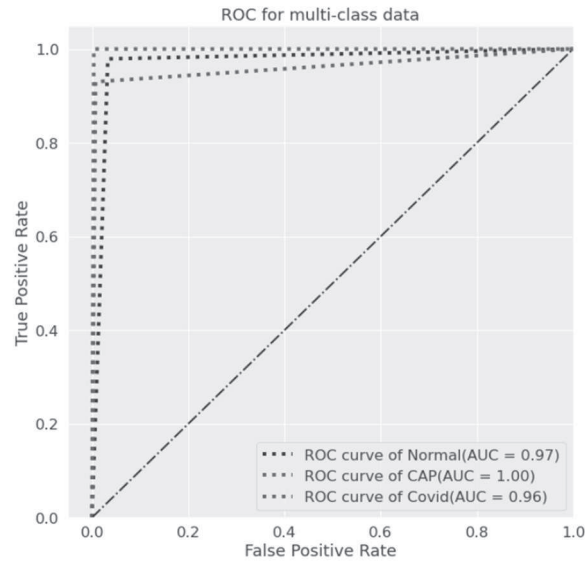


Fig 11: ROC curve based on DenseNet169 model.

4.1.3 Comparison of Confusion Matrix of different architectures.

Figure 12 shows Confusion Matrix, run for 25 epochs with ResNet50 Architecture whose model accuracy is 98.94% and loss is 4.06%.,

Figure 13 shows Confusion Matrix, run for 25 epochs with VGG16 Architecture whose model accuracy is 94.79% and loss is 5.21%.,

Figure 14 shows Confusion Matrix, run for 30 epochs with Densenet169 Architecture whose model accuracy is 97% and loss is 3.0%.

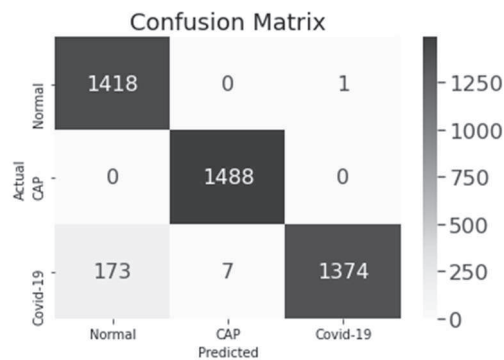


Fig 12: Confusion matrix based on Resnet50 model

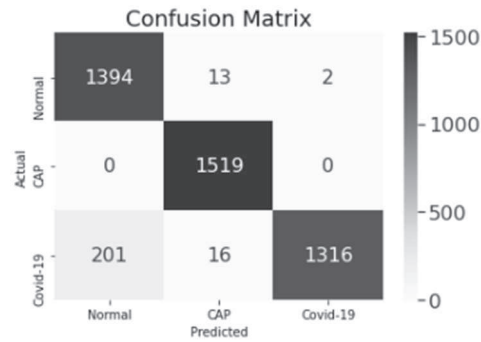


Fig 13: Confusion matrix based on VGG-16 model

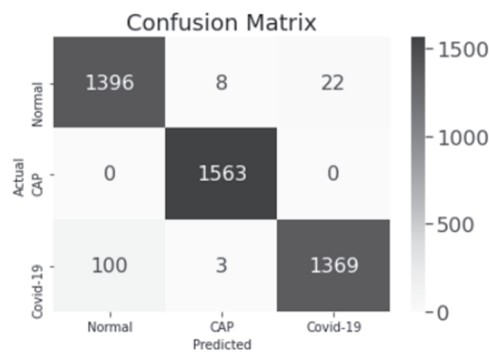


Fig 14: Confusion matrix based on DenseNet169 model.

4.2 SEGMENTATION

Numerous visual works, particularly in biomedical image processing where reliable segmentation of images is one of their key tasks since it requires us to characterize abnormal regions, the desired regions to be segmented, in addition to determining whether there is a disease. Selectivity must be included in the output, which necessitates giving each pixel a class label. The dataset is first split in two, 80:20 each between training and validation. To start segmenting the lungs, contrast limited adaptive histogram equalization was applied. After utilizing a preprocessing method to lessen noise and intensity inhomogeneity, all black slices were removed, and the region of interest that included the lungs was then clipped. Three kinds of the dataset’s images. Origin CT scans in the first ,Second : lung masking and Infection in the third column.

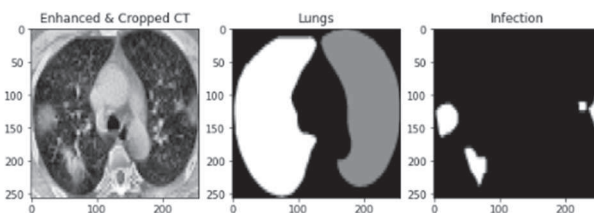


Fig 15: Mask of Lungs and Infection

After using U-Net Architecture input images is segmented semantically and instancally and compare with lung and infection mask which help for prediction taking threshold value of 0.5 which is shown in Figure 16 and Figure 17. The Unet Architecture model was used to segregate the infections and produce the infection masks. To determine the active infection that gives an estimate of the infection severity, the lung and infection region's area calculated.

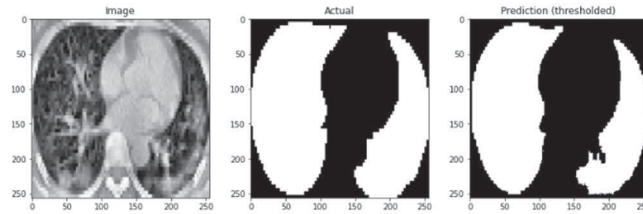


Fig 16: Prediction of Lungs Mask using U-Net Architecture.

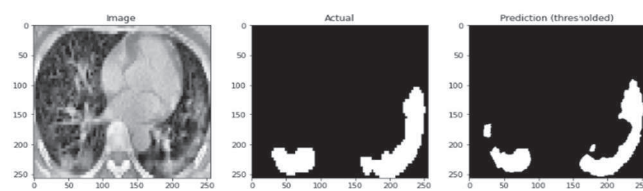


Fig 17: Prediction of Infection mask using U-Net Architecture

Dice similarity coefficient is a reproducibility validation measurement and an index of region. Here the lungs mask and infection mask also generate dice accuracy and loss during testing and validation after running of 30 epochs. Dice value for training for 30 epochs is 0.8245 and for validation is 0.7378 which is represented in Figure 18 and Figure 19.

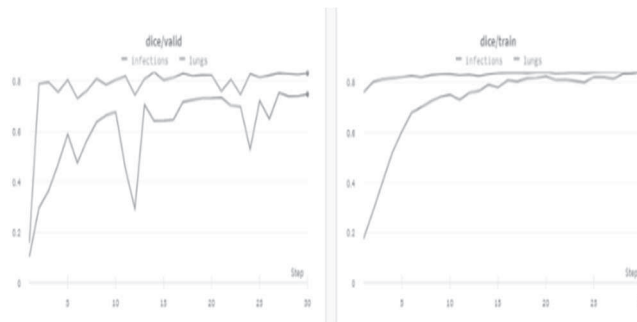


Fig 18: Dice Value of Lungs and Infection mask for Train and Validation.

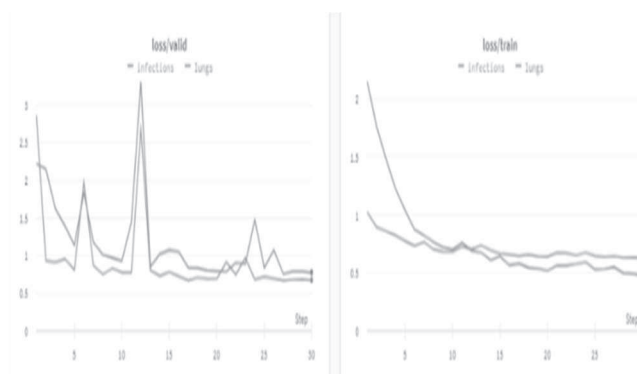


Fig 19: Dice loss of Lungs and Infection mask for Train and Validation.

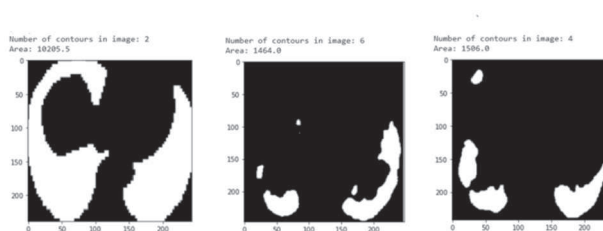


Fig 20: Calculation of the Area of Lung Mask and infection Mask

5. CONCLUSION

Using deep learning models like ResNet50, VGG-16, and DenseNet169, this research study intended to classify lungs CT images into COVID-19, CAP (Community-Acquired Pneumonia), and Normal categories. Techniques for Pre-processing were used to improve the image quality. Metrics including AUC, ACC, Precision, Recall, and F1 Score were taken into account for evaluation. In the second phase, lung CT scans were segmented using a U-Net architecture with an input size of 128x128 to find COVID-19-affected regions. Dice Score and IoU were used to evaluate the effectiveness of segmentation. The findings shown that predicted masks well matched real labels, even recognizing small infection spots. This study provides useful diagnostic tools for lung disorders, especially when it comes to separating COVID-19 and CAP from other CT Images.

6. FUTURE WORK

- Hardware and computational demands: Deep learning algorithms necessitate substantial computational resources, including high-performance GPUs, and their training can be time-intensive. Addressing these challenges is crucial for integrating deep learning in healthcare environments with limited resources.
- Future research should address the ethical and legal concerns associated with using deep learning algorithms for image analysis. These concerns revolve around patient privacy and data ownership, as medical images contain sensitive personal information. Developing robust frameworks to ensure privacy and secure data handling will be crucial for the responsible advancement of these technologies.

REFERENCES

- 1] Feng Shi, Jun Wang, Jun Shi, Ziyang Wu, Qian Wang, Zhenyu Tang, Kelei He, Yinghuan Shi, and Dinggang Shen. Review of artificial intelligence techniques in imaging data acquisition, segmentation, and diagnosis for covid-19. *IEEE reviews in biomedical engineering*, 14:4–15, 2020.
- 2] Ilker Ozsahin, Boran Sekeroglu, Musa Sani Musa, Mubarak Taiwo Mustapha, and Dilber Uzun Ozsahin. Review on diagnosis of covid-19 from chest ct images using artificial intelligence. *Computational and Mathematical Methods in Medicine*, 2020, 2020.
- 3] Wessam M Salama and Moustafa H Aly. Framework for covid-19 segmentation and classification based on deep learning of computed tomography lung images. *Journal of Electronic Science and Technology*, 20(3):100161, 2022.
- 4] Tao Ai, Zhenlu Yang, Hongyan Hou, Chenao Zhan, Chong Chen, Wenzhi Lv, Qian Tao, Ziyong Sun, and Liming Xia. Correlation of chest ct and rt-pcr testing for coronavirus disease 2019 (covid-19) in china: a report of 1014 cases. *Radiology*, 296(2):E32–E40, 2020.
- 5] Zhenyu Tang, Wei Zhao, Xingzhi Xie, Zheng Zhong, Feng Shi, Jun Liu, and Dinggang Shen. Severity assessment of coronavirus disease 2019 (covid-19) using quantitative features from chest ct images. *arXiv preprint arXiv:2003.11988*, 2020.
- 6] Liping Song, Xinyu Liu, Shuqi Chen, Shuai Liu, Xiangbin Liu, Khan Muhammad, and Siddhartha Bhattacharyya. A deep fuzzy model for diagnosis of covid-19 from ct images. *Applied Soft Computing*, 122:108883, 2022.
- 7] Hoon Ko, Heewon Chung, Wu Seong Kang, Kyung Won Kim, Youngbin Shin, Seung Ji Kang, Jae Hoon Lee, Young Jun Kim, Nan Yeol Kim, Hyunseok Jung, et al. Covid-19 pneumonia diagnosis using a simple 2d deep learning framework with a single chest ct image: model development and validation. *Journal of medical Internet research*, 22(6):e19569, 2020.
- 8] Aayush Jaiswal, Neha Gianchandani, Dilbag Singh, Vijay Kumar, and Manjit Kaur. Classification of the covid-19 infected patients using densenet201 based deep transfer learning. *Journal of Biomolecular Structure and Dynamics*, 39(15):5682–5689, 2021.
- 9] Sakshi Ahuja, Bijaya Ketan Panigrahi, Nilanjan Dey, Venkatesan Rajinikanth, and Tapan Kumar Gandhi. Deep transfer learning-based automated detection of covid-19 from lung ct scan slices. *Applied Intelligence*, 51:571–585, 2021.
- 10] Hemant Gunraj. Covid-19 ct scan dataset, 2022.
- 11] AndrewMVD. Covid-19 ct scans dataset, 2022.
- 12] S Vineth Ligi, Soumya Snigdha Kundu, R Kumar, R Narayanamoorthi, Khin Wee Lai, Samiappan Dhanalakshmi, et al. Radiological analysis of covid-19 using computational intelligence: a broad gauge study. *Journal of Healthcare Engineering*, 2022, 2022.
- 13] Mei-Ling Huang and Yu-Chieh Liao. A lightweight cnnbased network on covid-19 detection using x-ray and ct images. *Computers in Biology and Medicine*, 146:105604, 2022.
- 14] Moutaz Alazab, Albara Awajan, Abdelwadood Mesleh, Ajith Abraham, Vansh Jatana, and Salah Alhyari. Covid-19 prediction and detection using deep learning. *International Journal of*

Computer Information Systems and Industrial Management Applications, 12(June):168–181, 2020.

- 15] Pedro Silva, Eduardo Luz, Guilherme Silva, Gladston Moreira, Rodrigo Silva, Diego Lucio, and David Menotti. Covid-19 detection in ct images with deep learning: A voting-based scheme and cross-datasets analysis. *Informatics in medicine unlocked*, 20:100427, 2020.

Data Availability: <https://www.kaggle.com/datasets/divyaansingh/dataset15k/>